Mode Conversion and Design Consideration of Integrated Nonradiative Dielectric (NRD) Components and Discontinuities

François Boone and Ke Wu, *Senior Member, IEEE*

***Abstract*—In this paper, a class of nonradiative dielectric (NRD)-guide discontinuities is studied toward the establishment of design rules of NRD-guide circuits and components for millimeter-wave applications. A mode-matching technique with a multimodal transverse resonance condition is formulated to derive a generalized scattering matrix that allows accounting for effects of higher order modes and intermode coupling. Transmission properties of an NRD structure featuring a multilayered dielectric in cross section are presented. Mode conversion and power transfer among principal NRD-guide modes are, in particular, characterized for design consideration of NRD-guide components and circuits. New sets of easy-to-use design curves are introduced, thereby allowing practitioners to choose appropriate dielectric materials and NRD-guide topologies. Equivalent-circuit models are extracted from the generalized S-matrix for some basic and practically useful discontinuities involved in the design of almost every NRD-guide component, which include open ends, junctions, steps, and gaps. Calculated results of the selected structures are found to be in a good agreement with measurements. Dispersion diagrams of periodic NRD structures are also given in this paper.**

***Index Terms*—Computer-aided design, conversion, discontinuities, millimeter-waves, mode coupling, mode-matching method, nonradiative dielectric waveguide.**

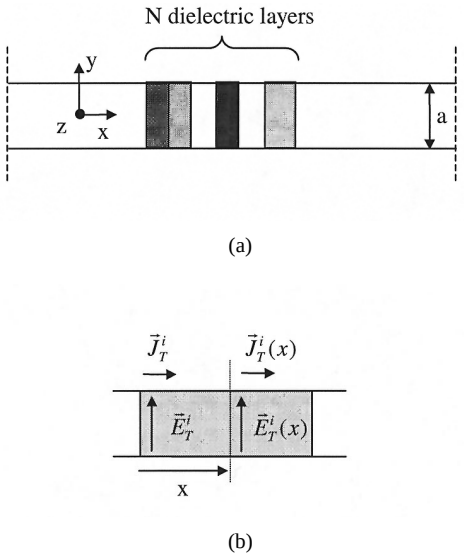

Fig. 1. Cross section view of a generalized NRD-guide. (a) Multilayered structure. (b) ith slice in the model.

I. Introduction

WIRELESS communications are being expanded into millimeter-wave range, which spark research interests in searching for low-cost and high-performance building blocks. Being successful in the realization of RF and microwave circuits and systems, hybrid and monolithic technologies still present the principal driving force behind the development of millimeter-wave circuits and systems on the basis of various forms of multilayered planar structure and microfabrication processing. In parallel, waveguide techniques have been widely used in the design of loss-sensitive building blocks such as filters and other passive components as the planar structure cannot fundamentally overcome its own transmission loss leading to undesirable low-Q performance. The nonradiative dielectric (NRD)-guide [1] is recognized as the first dielectric waveguide that has been found practically meaningful [2] in the low-cost and low-loss circuit design since it suppresses the inherent radiation loss of a dielectric waveguide and allows it to have sharp bends and other geometrical discontinuities. Such discontinuities are the foundation for the circuit design. Very recently, the hybrid integration technology [3], [4] of planar circuits and the NRD-guide has been proposed, which offers some unique possibility of exploring advantageous features of each structure in a combined scheme while offsetting the individual inherent shortcoming. Modeling and characterization of planar structure have been well documented as opposed to the NRD-guide whose design rules and electrical properties still need to be discussed in depth to achieve circuit optimization even though a number of NRD-guide components have been developed [5], [6].

To this end, a class of discontinuities commonly used in the design of NRD circuits and components are studied, and useful design databases are extracted from a mode-matching technique. This numerical scheme is formulated with a multimodal transverse resonance condition considering a multilayer cross section. A generalized S-matrix is derived for NRD discontinuities that allows accounting for effects of higher order modes and intermode coupling. Equivalent-circuit models

Manuscript received August 11, 1998. This work was supported by the Natural Sciences and Engineering Research Council of Canada.

F. Boone was with the Poly-Grames Research Center, Departement de Génie Électrique et de Génie Informatique, École Polytechnique de Montréal, C. P. 6079, Succ. Centre-Ville, Montreal, P.Q., Canada H3C 3A7 (e-mail: wuke@grmes.polymtl.ca). He is now with the Department of Electrical and Computer Engineering, University of Sherbrooke, Sherbrooke, P.Q., Canada J1K 2R1.

K. Wu is with the Poly-Grames Research Center, Departement de Génie Électrique et de Génie Informatique, École Polytechnique de Montréal, C. P. 6079, Succ. Centre-Ville, Montreal, P.Q., Canada H3C 3A7 (e-mail: wuke@grmes.polymtl.ca).

Publisher Item Identifier S 0018-9480(00)02787-3.

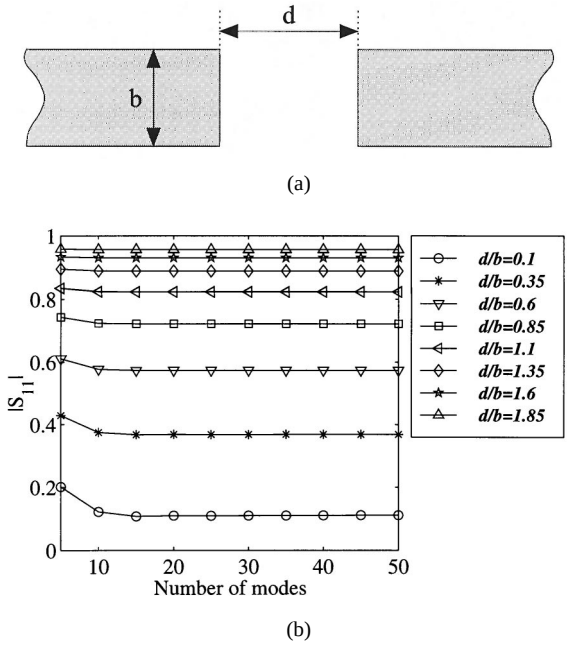

Fig. 2. Convergence behavior of results for an NRD gap discontinuity with $a = 5.00$ mm, $b = 3.556$ mm, $\varepsilon_r = 2.56$. (a) Air-gap discontinuity. (b) Reflection coefficient.

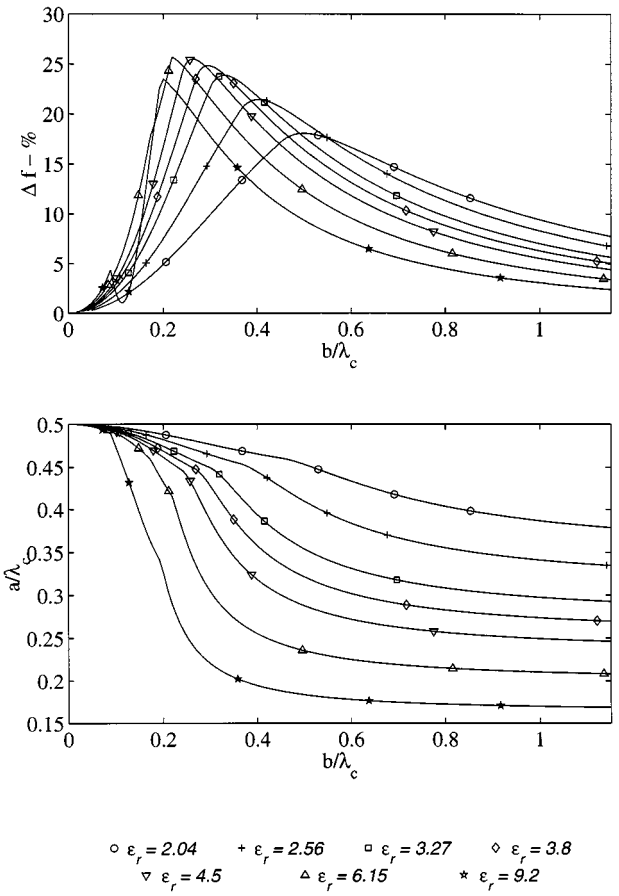

Fig. 3. Design curves for the optimal choice of geometrical parameters of the NRD-guide for a variety of dielectric materials: Teflon $\varepsilon_r = 2.04$, polystyrene $\varepsilon_r = 2.56$, TMM[3] $\varepsilon_r = 3.27$, quartz $\varepsilon_r = 3.8$, TMM[4] $\varepsilon_r = 4.5$, RT/Duroid 6006 $\varepsilon_r = 6.15$, TMM[9] $\varepsilon_r = 9.2$. (TMM and RT/Duroid 6006 are trademarks of the Rogers Corporation).

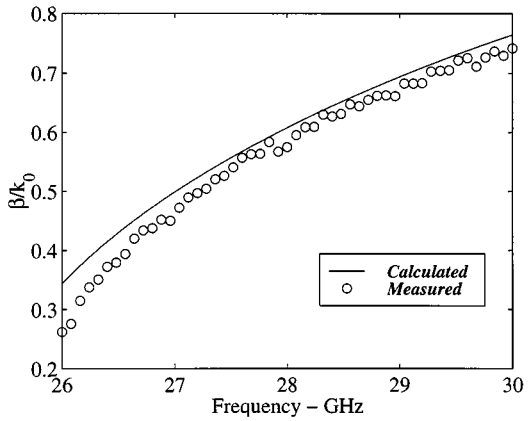

Fig. 4. Calculated and measured propagation constant for an NRD with $a = 5.00$ mm, $b = 3.556$ mm, and $\varepsilon_r = 2.56$.

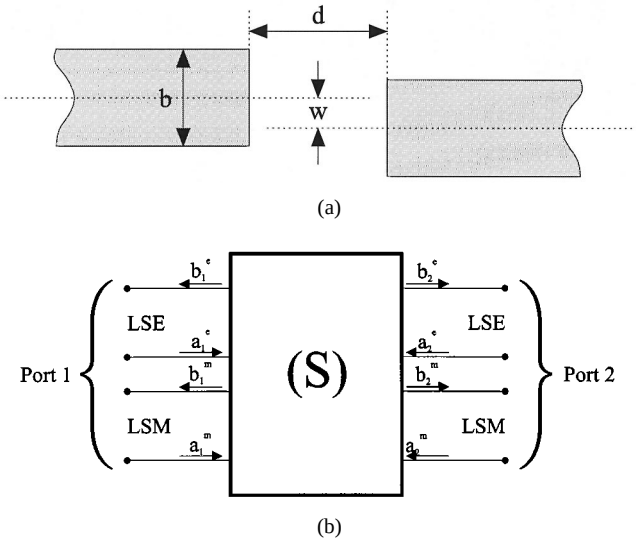

Fig. 5. Geometrical model and S-parameter model of the mode transfer or mode conversion for a generalized gap discontinuity. (a) Misalignment of a gapped dielectric discontinuity. (b) Parametric equivalence of LSM–LSE self-mode and intermode couplings.

are developed from calculated results for the purposes of design and optimization of basic discontinuity structures. The models are also validated by measurements for several typical discontinuities such as open ends. A dispersion diagram for periodic NRD structures are also developed.

II. Multimodal Transverse Resonance Theory

Fig. 1 shows the cross section of a generalized NRD-guide consisting of N-dielectric layers. The cross section is defined by the plane x–y and the wave propagation is along z axis. The spacing between the two metallic plates designated as "a" is slightly less than a half-wavelength in free space as required for the nonradiative waveguiding condition. In our modeling, the transverse section of the structure is terminated by metallic walls that are placed far enough from the dielectric part in order to avoid potential field interference. In fact, the analysis also allows having a complete unbounded cross section. A multimode transverse resonance technique (TRT) similar to [7] is applied to

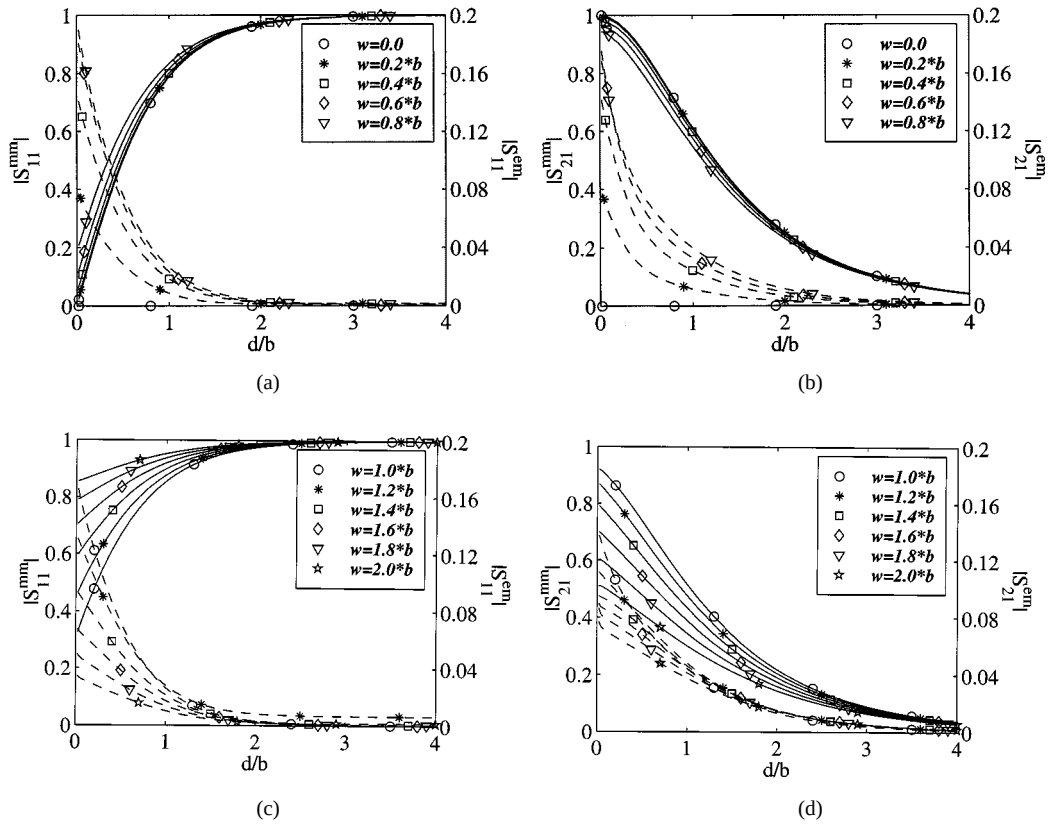

Fig. 6. Self-mode and intermode coupling characteristics in the case of an LSM–LSE mode conversion (backward and forward transmissions) considering various misaligned discontinuities with $a = 5.00$ mm, $b = 3.556$ mm, and $\varepsilon_r = 2.56$ (—: $|S_{ij}^{mm}|$. - - -: $|S_{ij}^{em}|$).

determine propagation constants for longitudinal section electric (LSE) and longitudinal section magnetic (LSM) modes in an exact manner. As for a mode numbered as "nth," the modal electric field $\vec{E}_T$ and the equivalent-current density $\vec{J}_T$ perpendicular to the cross section (tangential fields in parallel to the dielectric interfaces) are formulated for ith dielectric layer as follows:

$$\begin{pmatrix} \left|\vec{E}_T^i(x)\right\rangle \\ \left|\vec{J}_T^i(x)\right\rangle \end{pmatrix} = C_n^i(x) \begin{pmatrix} \left|\vec{E}_T^i\right\rangle \\ \left|\vec{J}_T^i\right\rangle \end{pmatrix} \tag{1}$$

in which $\vec{J}_T$ is defined by

$$\vec{J}_T = \sqrt{\frac{\mu_0}{\varepsilon_0}}\, \vec{H} \times \vec{x} \tag{2}$$

and

$$C_n^i(x) = \begin{pmatrix} ch(q_n x) & -j\,\dfrac{\lambda_n^\alpha}{q_n}\, sh(q_n x) \\ j\,\dfrac{q_n}{\lambda_n^\alpha}\, sh(q_n x) & ch(q_n x) \end{pmatrix} \tag{3}$$

with $\gamma^2 + \varepsilon_r^i k_0^2 + q_n^2 = (m\pi/a)^2$, where the symbol α refers to either LSE or LSM modes with $\lambda_n^{\mathrm{LSE}} = k_0$ and $\lambda_n^{\mathrm{LSM}} = -(q_n^2/\varepsilon_r^i k_0)$ and the subscript T refers to the plane y–z.

The x-oriented components of fields can simply deduced from Maxwell's equations $\nabla \cdot \vec{E} = 0$ and $\nabla \cdot \vec{H} = 0$. The field patterns and electrical description of the fundamental NRD modes can be found in [1] and [9]. The analytical knowledge of field expansion throughout the structure then allows the use of a mode-matching method or a multimode equivalent network approach, and then a generalized S-matrix can be derived for an NRD-guide discontinuity, as formulated in [8]. Useful design parameters characterizing the fundamental LSM_{10} mode can be extracted from this matrix such as insertion and return losses. The mode-matching method is usually known to have a relative convergence problem. This drawback is avoided in our modeling since the spacing of the metallic plates always remains unchanged according to the design principle of NRD-guide [1]. As shown in Fig. 2(a), the behavior of a simple convergence is described in Fig. 2(b) for the reflection coefficient of a gap discontinuity. The shorter the gap d becomes, the more important the influence of higher order modes will be. Therefore, the number of mode used in the modeling should be large enough to achieve the convergence. In any case, our analysis shows that 20 terms for LSE and LSM modes, respectively, seem to be largely sufficient for the required convergence and accuracy.

III. Critical Design Consideration and Waveguiding Propertries

A. Dimension Choice of NRD-Guide

To begin with, the conventional NRD-guide is used to showcase the dimension choice of NRD-guide even though it has been perceived as a matured procedure. Once a low-loss dielectric material is selected for the design and construction for

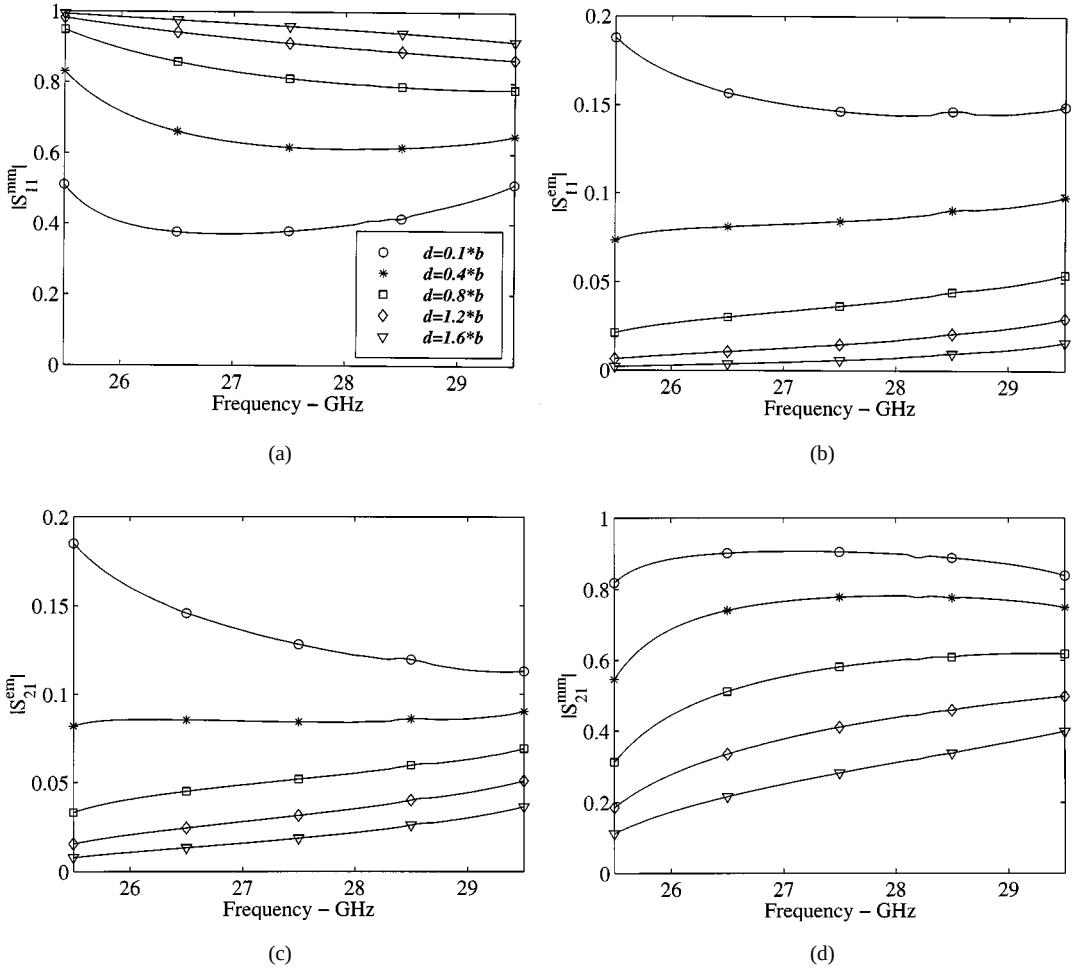

Fig. 7. Frequency response of the self-mode and intermode coupling effects for the LSM–LSE mode conversion in the case of the edge-to-edge offset discontinuity ($w/b = 1$).

a particular NRD-guide component, the optimal choice of the NRD-guide geometry such as cross-sectional dimensions is the first critical step toward optimized design of the NRD-guide component. In fact, the choice of an appropriate dielectric material available today is also much involved in it, which requires a concurrent design consideration. Design diagrams and some other useful curves were first introduced in [9] to characterize the effective monomode frequency bandwidth versus geometric dimensions for LSM_{10} operation. Nevertheless, the optimal choice of NRD-guide dimensions still remains difficult and not so obvious with the help of the characteristic curves given in [9] for two main reasons. First, the geometric dimensions of the NRD-guide are given only in a quotient form b/a so as to obtain a maximum frequency bandwidth. Second, the operating frequency center is also fixed by this quotient b/a, showing a very limited flexibility for the designer.

To make this procedure easier and convenient, we introduce in Fig. 3 a set of curves standing for a class of frequently used dielectrics. These curves that are related to the fractional bandwidth of frequency Δf and center frequency f_c (or wavelength λ_c) allow the user to quickly determine geometric dimensions of the NRD-guide for a given dielectric material. Let us choose f_c to begin with and one of the three characteristic parameters $\Delta f, a, b$; the most appropriate dielectric material can be selected from the curve reading and, subsequently, the two remaining unknown parameters can be determined to get the maximum frequency bandwidth available for the structure. In addition, such dimensions obtained from this procedure guarantee that only the first LSE_{10} mode and the fundamental mode LSM_{10} propagate along the NRD-guide. This is also a condition to minimize potential mode transfer or mode conversion between LSM to LSE, as will be shown later. At the very least, the seemly odd behavior of the characteristic curve for $\varepsilon_r = 9.2$ in the case of a small b/λ_c is caused by the suppression of a higher LSE mode in the fundamental-mode operating bandwidth.

An NRD-guide is now designed as an example for operating around $f_c = 28$ GHz. This guide is supposedly excited by an empty rectangular waveguide to NRD-guide transition. For a neat geometric matching between the two different guides, it may be common to choose the width b of the NRD-guide equal to the height b of the rectangular waveguide. In this case, the rectangular waveguide WR-28 is selected for use in this frequency range, which gives rise to $b = 3.556$ mm. As such, the ratio b/λ_c can be calculated and the optimum dielectric can be identified from the curves. In our case, a polystyrene dielectric block is used throughout this paper and its ε_r is approximately equal to 2.56. This gives us $a = 4.918$ mm with $\Delta f = 17.91\%$. To simplify the fabrication process, $a = 5.0$ mm is chosen

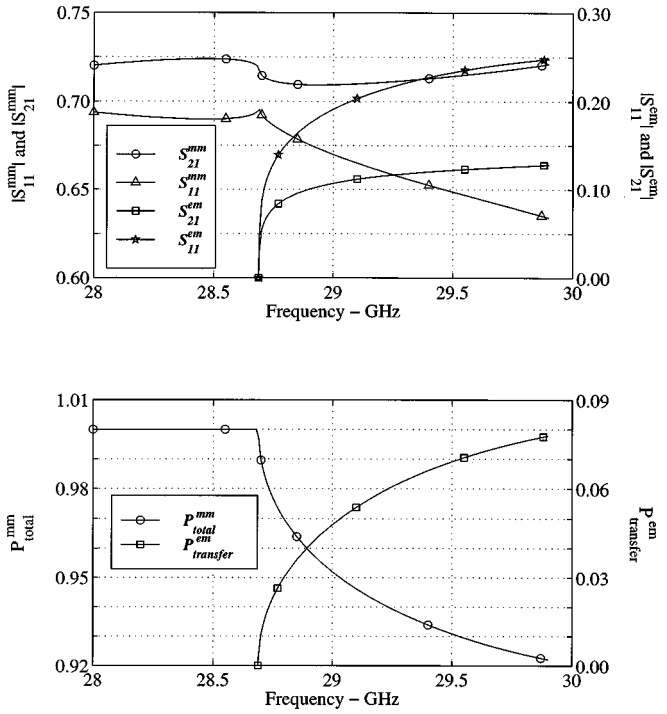

Fig. 8. Dispersion characteristics of the LSM_{10} to LSE_{11} mode and power transfers for a discontinuity with $w = 0$, $d = 0.5b$, $a = 5.00$ mm, $b = 5.00$ mm, and $\varepsilon_r = 2.56$.

TABLE I
CUTOFF FREQUENCIES IN GIGAHERTZ OF THE FIRST TWO MODES FOR THE NRD-GUIDE WITH $a = 5.00$ mm AND $b = 5.0$ mm AND $\varepsilon_r = 2.56$

m n	LSE_{mn}	LSM_{mn}
1 0	21.541	23.220
1 1	28.688	29.533

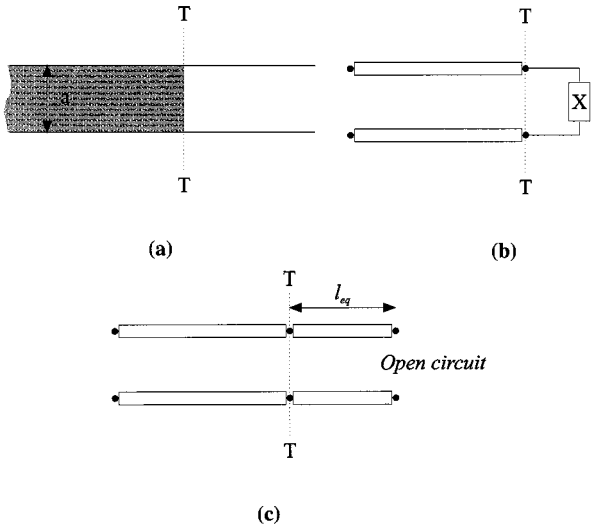

Fig. 9. Open-end discontinuity and circuit model of an NRD-guide. (a) Longitudinal geometry of the open-end discontinuity with $a = 5.00$ mm, $b = 3.556$ mm, and $\varepsilon_r = 2.56$. (b) Equivalent representation of a lumped reactance. (c) Equivalent representation of a line length.

and the resulting NRD-guide has a bandwidth of 17.53% and $f_c = 27.5819$ GHz. This outcome of the NRD-guide design will be used throughout this paper.

To validate our modeling technique and design procedure of the NRD-guide, a series of measurements are carried out to extract propagation constants of the designed 28-GHz NRD-guide. A pair of coax-to-rectangular waveguide-NRD guide transitions was used to launch the fundamental LSM_{10} mode with a thru-reflection line (TRL) deembedding procedure, as detailed in [10]. This TRL procedure allows us to not only extract S-parameters of a device-under-test (DUT), but also the propagation constant of the NRD-guide. Fig. 4 shows the calculated and measured results for the propagation constant, which are in good agreement over the frequency range of interest. The observable discrepancy may be caused by our low-precision of mechanical fabrication of the NRD-guide and its related testing block.

B. Intermode Coupling (Mode Conversion) Effect

The intermode coupling effect or mode conversion between two orthogonal fundamental modes presents one of the important guided-wave properties of the NRD-guide. In some cases, the power transfer happens inevitably from the fundamental LSM mode to its LSE counterpart if special NRD-guide discontinuities are encountered such as off-axial discontinuity or unbalanced or even asymmetric geometry along the waveguiding direction [11]. Generally speaking, all of the NRD-guide discontinuities are subject to this mode coupling effect, but may not always opt for it, depending on the input mode excitation or NRD coupling mechanism. This mode conversion effect may be characterized by a transmission loss for the fundamental mode, which may be harmful in some applications (e.g., misalignment) or useful in the others (e.g., power division), depending on the circumstances. Fig. 5(a) depicts two NRD-guide lines that are not aligned axially, but with some offset in the cross-sectional direction.

In the case of a mode conversion, both modes fulfill the guiding condition along the NRD-guide structure and its equivalent model should be regarded as a network of four ports with modal incident and reflected waves, as shown in Fig. 5(b). The intermode coupling can be judged by a 4×4 scattering matrix with two pair of incident and reflected waves as follows:

$$\begin{pmatrix} b_1^e \\ b_1^m \\ b_2^e \\ b_2^m \end{pmatrix} = \begin{pmatrix} S_{11}^{ee} & S_{11}^{em} & S_{12}^{ee} & S_{12}^{em} \\ S_{11}^{me} & S_{11}^{mm} & S_{12}^{me} & S_{12}^{mm} \\ S_{21}^{ee} & S_{21}^{em} & S_{22}^{ee} & S_{22}^{em} \\ S_{21}^{me} & S_{21}^{mm} & S_{22}^{me} & S_{22}^{mm} \end{pmatrix} \begin{pmatrix} a_1^e \\ a_1^m \\ a_2^e \\ a_2^m \end{pmatrix}. \quad (4)$$

Therefore, the generation of such a matrix is the most critical issue in the understanding of mode conversion and power transfer between the LSM_{10} (with the superscript "m") and LSE_{10} (with "e") modes. In our case, the mode conversion and power transfer from LSM_{10} to LSE_{10} are especially studied even though the reverse case can be made in a very similar way. As indicated in Fig. 5(b), the intermode coupling can be classified into two categories: forward and backward couplings, which are characterized by (S_{21}^{me}, S_{21}^{em}) or (S_{12}^{me}, S_{12}^{em}) and (S_{11}^{me}, S_{11}^{em}) or (S_{22}^{me}, S_{22}^{em}). The reciprocal properties and energy conservation theorems are applied to this lossless case.

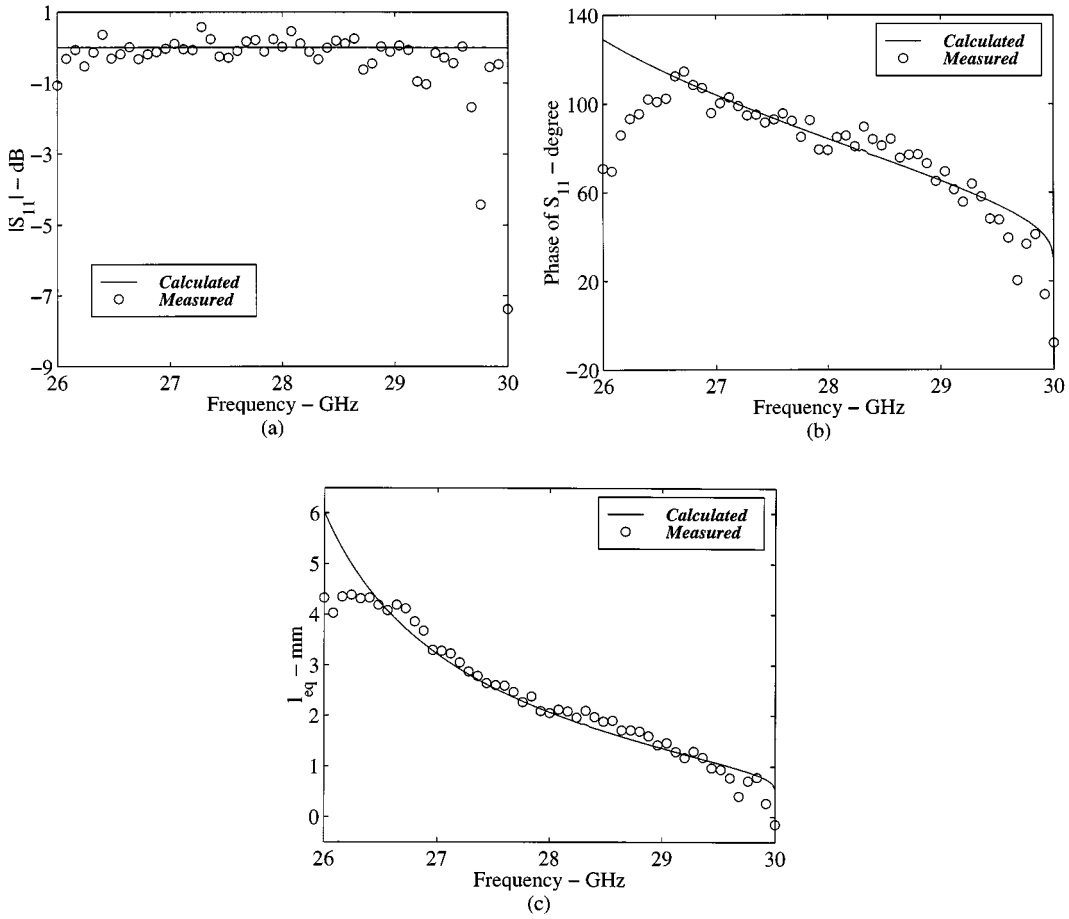

Fig. 10. Calculated and measured results of S-parameters for the NRD open-end discontinuity. (a) Amplitude of the reflection coefficient. (b) Phase of the reflection coefficient. (c) Extracted l_{eq} for the equivalent model.

Fig. 6 shows a set of characteristic curves of selected scattering parameters obtained at 28 GHz from the generalized S-matrix for intermode and self-mode couplings. The results are generated as a function of the normalized gap ratio d/b versus the normalized offset parameter (or misalignment) w/b. It indicates that the intermode coupling is rather strong as long as w/b remains smaller than 1.0. No coupling occurs between the two modes in the case of $w/b = 0$ because the two modes are in the state of orthogonality. In any case, this strong coupling happens for a misaligned small gap (usually $d/b < 1.5$). This observation is applied to all the cases regardless of the forward or backward coupling. Such a coupling becomes monotonically reduced with w/b and d/b for the case of $w/b > 1$. The intermode coupling may be negligible once the parameter d/b is greater than 2.0, standing for a large gap. Interestingly, the maximum intermode coupling takes place around $w/b = 1$, otherwise it is decreased in a gradual manner. This phenomenon suggests that the LSM_{10} mode should effectively be converted into its LSE counterpart if the exact offset (edge-to-edge or $w/b = 1$) arrangement of two NRD-guides is made. Such a unique feature of mode conversion is rather important for the design of NRD-guide power dividing and combining components. In addition, our results indicates the necessity of using a field-theory-based package for the NRD-guide component design if an offset geometry is involved, which is subject to a significant mode conversion at both input and output ports.

It is found in Fig. 6 that the self-mode coupling (reflection and transmission) is quite as usual, except for the offset influence. This influence is much more pronounced for $w/b > 1$. In any case, the LSM_{10} mode transmission and reflection coefficients are significantly affected for a small gap and the mode power will be completely reflected back once d/b goes beyond 2.0. The two NRD-guides are then independent, and the mode conversion disappears completely.

To complement our discussion, Fig. 7 shows frequency responses of the S-parameters depicting the self-mode and intermode coupling in the case of the edge-to-edge offset discontinuity ($w/b = 1$). Such curves indicate that the intermode coupling behaves relatively flatly over the bandwidth of interest, and it can be enhanced as the height of an NRD-guide is close to its wavelength limiting value. As previously discussed, the intermode coupling decreases as d/b increases, and the structure exhibits predominantly a self-mode coupling effect.

Let us now have a close look at the effect of mode conversion to the second LSE mode, namely, LSM_{10} to LSE_{11} for $w/b = 0$, $d/b = 0.5$, $a = b = 5.0$ mm. The choice of $w/b = 0$ guarantees the absence of a coupling between the two fundamental modes LSE_{10} and LSM_{10} because of the modal orthogonality. In the proximity of a discontinuity, the intermode coupling or mode conversion between LSE_{11} and LSM_{10} will take place. Note that the modes LSE_{10} and LSE_{11} are different

in field profile. Table I gives the cutoff frequencies in gigahertz for the selected NRD-guide for the first guided-modes, indicating that the potential intermode coupling can occur only if the operating frequency is higher than the cutoff frequency of LSE_{11} mode (28.688 GHz). The power conservation for LSM_{10} mode is simply described with normalized terms by the following equation if $f < 28.688$ GHz:

$$P_{\mathrm{total}}^{mm} = |S_{11}^{mm}|^2 + |S_{21}^{mm}|^2 = 1 \tag{5}$$

and the power transfer $P_{\mathrm{transfer}}^{em}$ is equal to zero. Fig. 8 displays two pairs of graphs showing the frequency response of the intermode coupling or mode conversion from LSM_{10} to LSE_{11}. It can be observed that (5) is no longer valid for the LSM_{10} mode once the NRD-guide is used at frequency larger than 28.688 GHz and the power transfer increases and reaches a maximum of 7.79%. The mode conversion from LSM_{10} to LSE_{11} is well characterized by the behavior change in characteristic parameters such as S_{11}^{em} and S_{21}^{em}, while S_{11}^{mm} and S_{21}^{mm} are subject to an abrupt power loss around the cutoff frequency and then exhibit smooth frequency response with a continued signal loss.

C. NRD-Guide Open-End Effect

The open end of an NRD-guide is one of the geometrical discontinuities, as shown in Fig. 9(a), which is frequently encountered in the design of passive components and active devices. In this example, the cross section of the NRD-guide is characterized by $a = 5.0$ mm and $b = 3.556$ mm. Similar to that of a planar transmission line, dispersive fringing effects of the open end can be represented or extracted by a lumped reactance modeled as a shunt susceptance [see Fig. 9(b)]. This susceptance may exhibit either a capacitance for the LSE mode or an inductance for the LSM mode, which establishes the reference plane for an electrically ideal open end. This is usually done by extending an effective length of the same NRD strip to simulate such capacitive or inductive effects, as indicated in Fig. 9(c). This effective (or equivalent) length l_{eq}, which is useful for the design consideration of NRD-guide components, can be obtained for the fundamental LSM_{10} mode, e.g., by

$$l_{\mathrm{eq}} = \frac{\arg(\Gamma)}{2\beta_{\mathrm{LSM}}} \tag{6}$$

in which Γ is the reflection coefficient measured or calculated at the physical plane of open end in question. Measured and calculated amplitude and phase of S_{11} at the plane of the open end are plotted in Fig. 10(a) and (b), respectively. It can be seen that errors of measurement are well observed over the frequency range of interests. In particular, the 26.5-GHz cutoff effect of the mode launcher from the rectangular waveguide causes to a large extent of the phase deviation, and also the fabrication tolerance and calibration errors, may contribute to the mismatch between the two results, which, however, are found to be in good agreement. The difference of results around the upper part of the frequency range may come from the fact that a is very close to the spacing limitation governed by the nonradiative condition of the guide, which is a half-wavelength in free space, or other unknown factors. In any case, the calculated effective length l_{eq}, as shown in Fig. 10(c), is very close to the measured one, thereby validating our model.

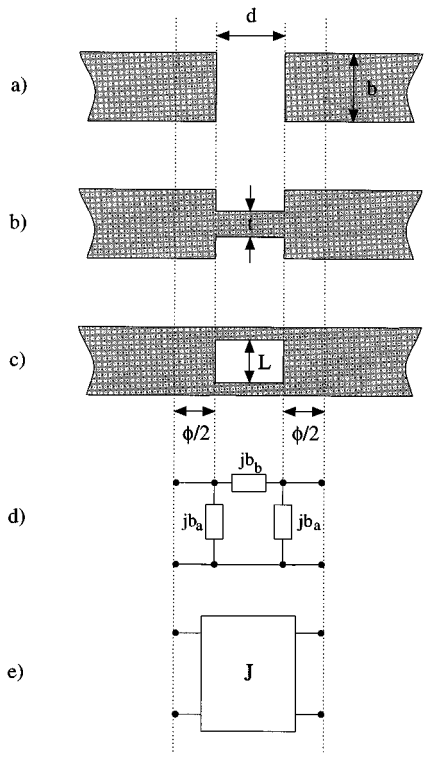

Fig. 11. Three typical discontinuities frequently encountered in the design of NRD circuits and components. The NRD-guide is determined by $a = 5.00$ mm, $b = 3.556$ mm, $\varepsilon_r = 2.56$. (a) Air-gap discontinuity. (b) Double-step discontinuity with a width t for the coupling section. (c) Notch discontinuity with $L = b - t$. (d) π-equivalent circuit for LSM_{10} mode. (e) Equivalent J-inverter.

D. Electrical Characteristics of Typical NRD-Guide Discontinuities

There are so many varieties of NRD-guide discontinuities that our study is only centered herewith on three basic discontinuities, as shown in Fig. 11, for an NRD-guide with a cross section of $a \times b = 5.0 \times 3.556$ mm^2. The structures, namely: 1) air gap discontinuity; 2) double-step discontinuity; and 3) notch discontinuity, are some fundamental building blocks of a large number of passive components, in particular, in the design of filters. Generally speaking, the double step and notch discontinuities share almost the same guided-wave behavior. As the dielectric thickness t becomes large or the notch width ($L = b - t$) is narrow in the coupling section, both LSE_{10} and LSM_{10} modes can propagate along it as a normal transmission line and the discontinuity effects of the structures are much less pronounced. Oppositely, the two modes are evanescent and coupling between the interconnected two NRD-guides is realized by such evanescent modes similar to the air-gap case of Fig. 11(a). In this case, the coupling section may be better characterized by designer-friendly K- or J-inverter parameter [12], as described

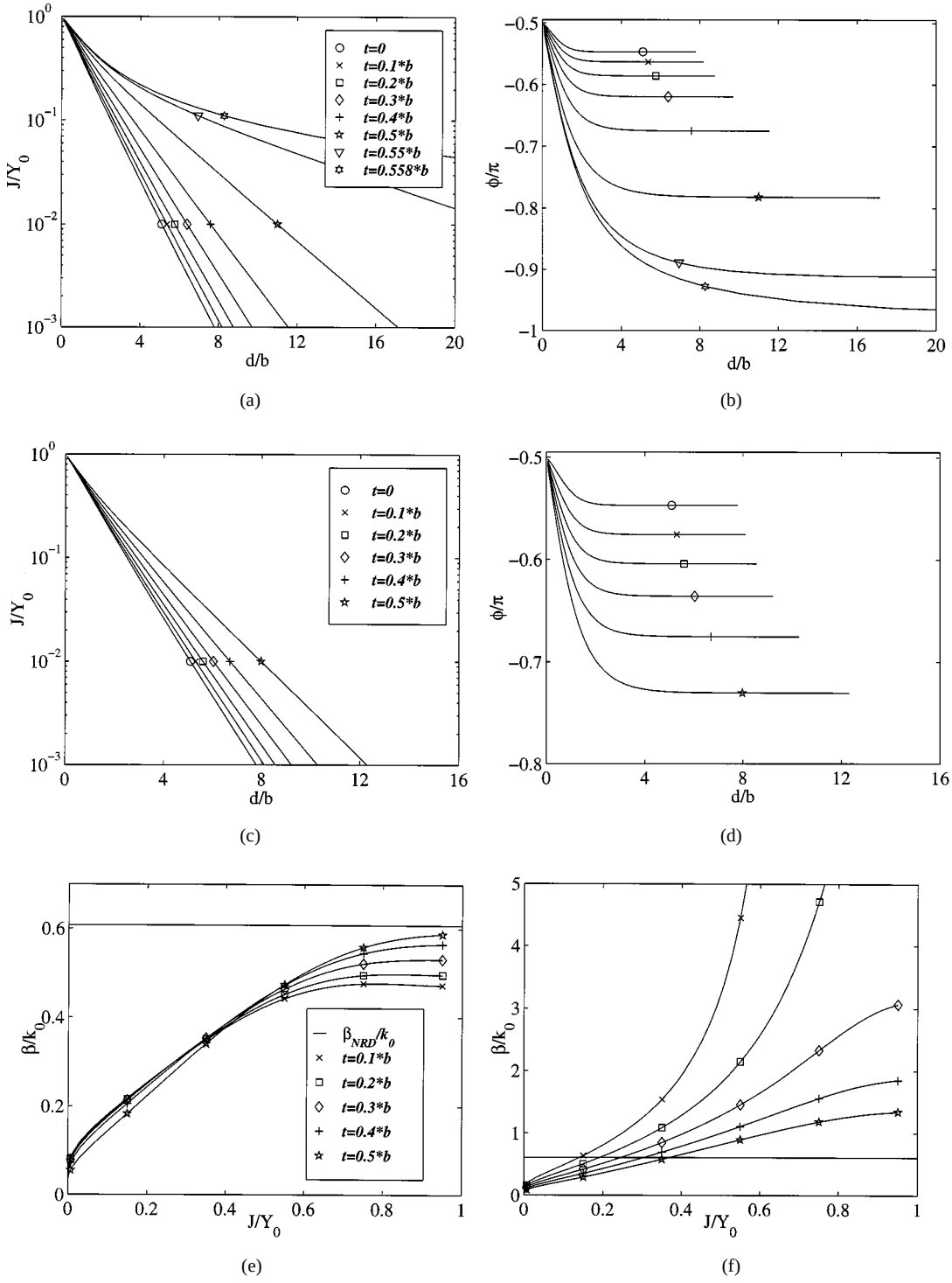

Fig. 12. Equivalent parameters for the J-inverter extracted for the discontinuities. (a) and (b) J and ϕ parameters for the double-step discontinuity. (c) and (d) J and ϕ parameters for the notch discontinuity. (e) and (f) β/k_0 design curves for the mode coupling.

by Fig. 11(e). J (admittance inverter parameter) and ϕ (equivalent length) are calculated as a function of d/b on the basis of LSM_{10} π-equivalent circuit see [Fig. 11(d)] by

$$J = Y_0 \left| \tan\left(\frac{\phi}{2} + \tan^{-1}\left(\frac{b_a}{Y_0} \right) \right) \right| \tag{7}$$

$$\phi = -\tan^{-1}\left(\frac{2b_b}{Y_0} + \frac{b_a}{Y_0} \right) - \tan^{-1}\left(\frac{b_a}{Y_0} \right) \tag{8}$$

where Y_0 is the characteristic admittance of the NRD guide.

Fig. 12(a) and (b) gives two groups of the design curves for J/Y_0 and ϕ values, respectively, of double-step discontinuities, which also involve the air-gap discontinuity case ($t = 0$). It can be expected that the inverter parameter shows exponential decays versus d/b, for which a larger thickness t brings up more reactance effects, which can be read very well in Fig. 12(b). Nevertheless, the critical value of t is found to be equal to $0.55835 \times b$ mm in our example, for which the boundary line of coupling and propagation between the input and output ports

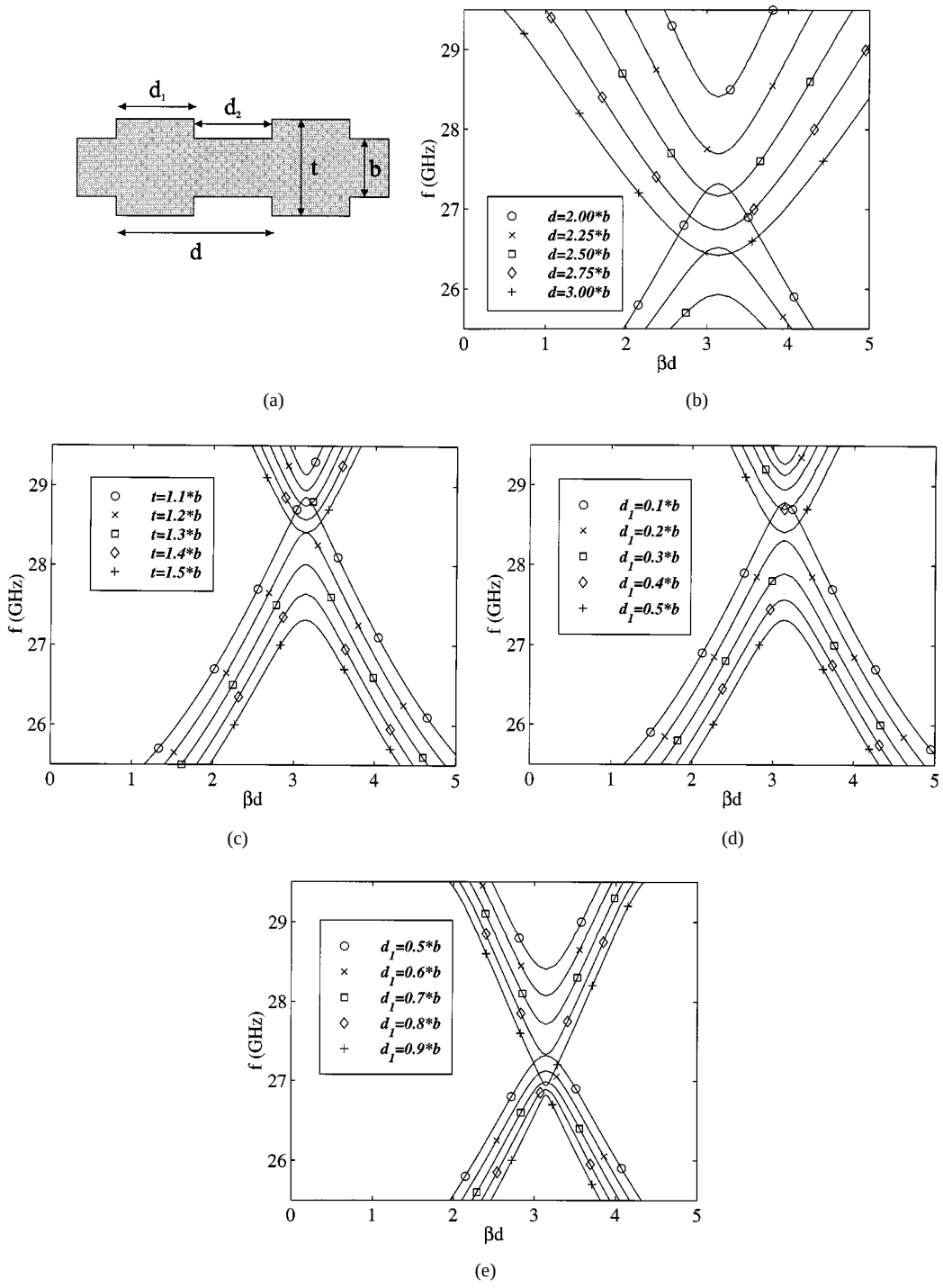

Fig. 13. Dispersion diagram $f - \beta$ for NRD-guide periodic structures. In all cases, the NRD-guide dimensions are $a = 5.00$ mm and $b = 3.556$ mm and $\varepsilon_r = 2.56$. (a) Geometrical view of the periodic structures. (b) $d_1 = d_2 = d/2, t = 1.5b$. (c) $d_1 = d_2 = b$. (d) $d_1 + d_2 = 2b, t = 1.5b$. (e) $d_1 + d_2 = 2b$, $t = 1.5b$.

can be identified through evanescent modes or guided-modes. This is an important feature for the design of filters and other passive components. Similar results can be generated for a number of notch discontinuities with $L = b - t$, as shown in Fig. 12(c) and (d), for which the critical value of t is found to be $0.65100 \times b$ mm.

In the case of an NRD-guide filter design, to name an example, the filter prototype constraints usually yield a set of predesignated constants J/Y_0 regardless of the filter topology. For example, the typical inverter parameters for a five-pole filter operating at 28 GHz with a 3% bandwidth are $J_{01}/Y_0 = J_{56}/Y_0 = 0.4507$, $J_{12}/Y_0 = J_{45}/Y_0 = 0.1858$, and $J_{23}/Y_0 = J_{34}/Y_0 = 0.1416$. While keeping the same set of J/Y_0 values, it is rather flexible for practitioner to choose an appropriate NRD-guide coupling section. It is easy to predict from the design curves that a differential change of the filter topology produces simultaneous incremental offsets Δd and $\Delta\phi$ in length d of the coupling section and in equivalent length

ϕ of the extracted J-inverter. It can then be justified that the filter size can be reduced if and only if

$$\beta_{\mathrm{NRD}} < \beta_{\mathrm{eff}} \tag{9}$$

where β_{NRD} denotes the propagation constant of the NRD-guide at center frequency of the design, and the new parameter β_{eff} is defined by the following differential term:

$$\beta_{\mathrm{eff}} = -\frac{\Delta\phi}{\Delta d}. \tag{10}$$

Some useful results for $\beta_{\mathrm{eff}}k_0$ are plotted in Fig. 12(e) for the double-step discontinuity and Fig. 12(f) for the notch discontinuity. In our example, the center frequency is 28 GHz and β_{NRD}/k_0 is then 0.6079. The derived curves point out that, on one hand, a filter designed with the double-step discontinuity coupling scheme always presents a longer size than with the air-gap discontinuity section. In a practical design, the former coupling structure seems to be a judicious choice over the latter since this structure-based filter has a single dielectric block free from any alignment problem and the unwanted LSM_{10} to LSE_{10} mode conversion or power transfer loss can effectively be avoided. On the other hand, a design on the basis of the notch discontinuity can be shorter than other filter topologies, and this structure poses no misalignment problem. This design consideration is significant in minimizing the filter size. Such a size reduction merits some special attention in the choice of a suitable coupling section for transmission loss reduction at millimeter-wave frequency.

Infinite periodic-grating NRD-guide structures are found useful for filter design or other use, in particular, in the prediction of passband and stopband locations over the frequency range of interest. An NRD-guide ring may be periodically loaded with stubs, which presents a typical example for the suppression of potential spurious resonance. In this case, for a periodic NRD-guide of Fig. 13(a) with the same cross section as the above-described examples, Floquet's theorem is applied to obtain the $f-\beta$ dispersion diagram, as shown in Fig. 13(b)–(e). Other parameters are variable such as t, d_1, d_2, and $d = d_1 + d_2$. These design curves indicate some interesting parametric influence on the stopband characteristics of the periodic structure.

IV. Conclusion

In this paper, a generalized S-matrix technique of NRD-guide discontinuities and components is derived from a mode-matching technique with a transverse resonance scheme, considering high-order mode coupling and power transfer. Some important properties of NRD-guide discontinuities are revealed for design consideration. Useful design feature and rules are extensively discussed and presented for frequently used structures with a large number of design curves and diagrams. In particular, a design principle in the choice of an appropriate NRD-guide is proposed for designer to choose the best possible geometry per dielectric material. Mode conversion and power transfer from LSM_{10} to LSE_{10} and LSE_{11} are studied in detail and single-block-coupling structures are proposed to avoid any potential misalignment problem in the axial direction. New characteristic parameters are introduced in minimizing the size of an NRD-guide circuit. Dispersion $f-\beta$ diagrams are also presented for the design purpose of a periodic NRD-guide with emphasis on frequency response.

Acknowledgment

The authors would like to thank one of the reviewers for the useful comments that resulted in the improvement of this paper in many aspects.

References

[1] T. Yoneyama and S. Nishida, "Nonradiative dielectric waveguide for millimeter wave integrated circuits," *IEEE Trans. Microwave Theory Tech.*, vol. MTT-29, pp. 1188–1192, Nov. 1981.

[2] A. A. Oliner, "Historical perspectives on microwave field theory," *IEEE Trans. Microwave Theory Tech.*, vol. MTT-32, pp. 1022–1045, Sept. 1984.

[3] K. Wu and L. Han, "Hybrid integration technology of planar circuits and NRD guide for cost effective microwave and millimeter-wave applications," *IEEE Trans. Microwave Theory and Tech.*, vol. 45, pp. 946–954, June 1997.

[4] K. Wu, *Hybrid Three-Dimensional Planar/Nonplanar Circuits for Microwave and Millimeter-Wave Applications: The State of the Art and Challenge*. Nis, Yugoslavia: Facta Univ., 1998, vol. 11, pp. 87–101.

[5] T. Yoneyama and S. Nishida, "Nonradiative dielectric waveguide circuit components," *Int. J. Infrared Millim. Waves*, vol. 4, pp. 439–449, 1983.

[6] J. F. Miao, "Studies of NRD waveguide in China," in *PIERS 1997*, vol. 1, Hong-Kong, p. 203.

[7] T. Itoh, *Numerical Techniques For Microwave And Millimeter-Wave Passive Structures*. New York: Wiley, 1989.

[8] A. S. Omar and K. Schünemann, "Transmission matrix representation of finline discontinuities," *IEEE Trans. Microwave Theory Tech.*, vol. MTT-33, pp. 765–770, Sept. 1985.

[9] T. Yoneyama, "Nonradiative dielectric waveguide," *Int. J. Infrared Millim. Waves*, vol. 11, pp. 61–98, 1984.

[10] D. Rubin, "De-embedding mm wave MIC's with TRL," *Microwave J.*, pp. 141–150, June 1990.

[11] S. Xu, X. Wu, and T. Yoneyama, "Scattering properties of discontinuities in NRD guide," *Proc. Inst. Elect. Eng.*, vol. 141, no. 3, pp. 205–210, June 1994.

[12] G. Matthaei, L. Young, and E. M. T. Jones, *Microwave Filters, Impedance-Matching Networks, and Coupling Structures*. Norwood, MA: Artech House, 1980.

François Boone was born in Dijon, France. He received the Eng.Dipl. degree in electrical engineering from École Nationale Supérieure d'Électronique, d'Électrotechnique, d'Informatique et d'Hydraulique de Toulouse (ENSEEIHT), Toulouse, France, in 1992, the DEA degree in microwave engineering from the Institut National Polytechnique de Toulouse (INPT), Toulouse, France, in 1993, and the M.Sc.A and Ph.D. degrees in microwave engineering from the École Polytechnique de Montréal, Montréal, Canada, in 1997 and 2000, respectively.

In October 1999, he joined the faculty of the Department of Electrical and Computer Engineering, University of Sherbrooke, Sherbrooke, P.Q., Canada, where he is currently an Assistant Professor. His main research interests concern analysis, modeling, and design of passive and active microwave and millimeter-wave components and circuits.

Ke Wu (M'87–SM'92) was born in Liyang, Jiangsu Province, China. He received the B.Sc. degree with distinction in radio engineering from the Nanjing Institute of Technology (now Southeast University), Nanjing, China, in 1982, and the D.E.A. and Ph.D. degree with distinction in optics, optoelectronics, and microwave engineering from the Institut National Polytechnique de Grenoble (INPG), Grenoble, France, in 1984 and 1987, respectively.

He conducted research in the Laboratoire d'Electromagnetisme, Microondes et Optoelectronics (LEMO), Grenoble, France, prior to joining the Department of Electrical and Computer Engineering, University of Victoria, Victoria, B.C., Canada. He subsequently joined the Department of Electrical and Computer Engineering, Ecole Polytechnique de Montréal (Faculty of Engineering, University of Montréal), Montreal, Canada, as an Assistant Professor, and is currently a Full Professor. He held a 1995 Visiting Professorship in France (Telecom-Paris and INP-Grenoble), a 1996-1997 Visiting Professorship at the City University of Hong Kong, a 1999 Guest Professorship at the Swiss Federal Institute of Technology (ETH-Zürich), Zürich, Switzerland, as well as several short-term Visiting Professorships at other universities. He also holds an Honorary Visiting Professorship at the Southeast University, China. He is currently a Visiting Professor at the National University of Singapore. He has been the Head of the FCAR Research Group of Quebec, where he is involved with RF and millimeter-wave electronics, and the Acting Director of the Poly-Grames Research Center. He has authored or co-authored over 250 referred journal and conference papers and several book chapters. His current research interests involve three-dimensional (3-D) hybrid/monolithic planar and nonplanar integration techniques, active and passive circuits, antenna arrays, advanced field-theory-based CAD and modeling techniques, and development of low-cost RF and millimeter-wave transceivers. He is also interested in the modeling and design of microwave photonic circuits and systems. He was chairperson of the 1996 ANTEM Publicity Committee and vice-chairperson of the Technical Program Committee (TPC) for the 1997 Asia–Pacific Microwave Conference (APMC'97). He has served on the FCAR Grant Selection Committee (1993–1996, 1998–1999), and the TPC committee for the TELSIKS and ISRAMT. He has also served on the ISRAMT International Advisory Committee. He was the general co-chair of the 1999 SPIE International Symposium on Terahertz and Gigahertz Photonics, Denver, CO. He serves on the Editorial Review Board for *Microwave and Optical Technology Letters*.

Dr. Wu is a member of the Electromagnetics Academy. He has served on the Editorial or Review Boards of various technical journals, including the IEEE TRANSACTIONS ON MICROWAVE THEORY AND TECHNIQUES, the IEEE TRANSACTIONS ON ANTENNAS AND PROPAGATION, and the IEEE MICROWAVE AND GUIDED WAVE LETTERS. He served on the 1996 IEEE Admission and Advancement (A&A) Committee and the Steering Committee for the 1997 joint IEEE APS/URSI International Symposium. He has also served as a TPC member for the IEEE Microwave Theory and Techniques Society (IEEE MTT-S) International Microwave Symposium. He received a URSI Young Scientist Award, the Institute of Electrical Engineers (IEE) Oliver Lodge Premium Award, the Asia–Pacific Microwave Prize Award, the University Research Award "Prix Poly 1873 pour l'Excellence en Recherche," presented by the Ecole Polytechnique on the occasion of its 125th anniversary, and the Urgel-Archambault Prize (the highest honor) in the Field of Physical Sciences, Mathematics and Engineering from the French-Canadian Association for the Advancement of Science (ACFAS).